Two Kinds of Polarization Filter Based on Photonic Crystal Fiber With Nanoscale Gold Film

Qiang Liu
Shuguang Li
Hailiang Chen, Student Member, IEEE

Two Kinds of Polarization Filter Based on Photonic Crystal Fiber With Nanoscale Gold Film

Qiang Liu, Shuguang Li, and Hailiang Chen, *Student Member, IEEE*

Key Laboratory of Metastable Materials Science and Technology, College of Science,
Yanshan University, Qinhuangdao 066004, China

Abstract: The polarization characteristics of photonic crystal fibers (PCFs) with nanoscale gold film are evaluated by using a finite element method. The coupling theory between core mode and SPP mode is introduced. Their application to fiber filter is investigated. The PCF filters for the ranges of 1.31, 1.48, and 1.55 μm and a wide wavelength range are designed. We demonstrate that the resonance wavelengths are modulated by adjusting the diameter of the air hole with gold film, and the resonance wavelengths of x-polarized and y-polarized mode are divided by high birefringence of core. By our structure, the loss of y-polarized mode is larger than the loss of x-polarized mode at the resonance wavelength. When the diameter of the air hole with gold film is big enough, the loss of y-polarized mode is further larger than the loss of x-polarized mode at the wavelength range of 1.25–2.0 μm.

Index Terms: Photonic crystal fiber, polarization filter.

1. Introduction

Photonic crystal fibers (PCFs), which are also called holey fibers or microstructured optical fibers, are consist of periodic array air holes parallel to the propagation axis [1]. The light is confined in the defects of the periodic structure. PCFs are divided into two kinds of fibers. The first one, i.e., index-guided PCF, guides light by total internal reflection between a high refractive index core and a low refractive index cladding region. The other one, i.e., photonic-bandgap PCF, guides light by the photonic bandbag in a low refractive index core-region. In this paper, index-guided PCF is employed. PCFs reveal many advantages, such as high-birefringence [2], low loss [3], big mode area [4], and so on. The characteristics of PCF could be extended by filling the cladding air holes with liquid [5], liquid crystal [6], metal [7], oil [8], and so on. PCFs with metal wires or metal film arouse our interests. Surface plasmon polaritons (SPPs) can form on the surface of metal when they are stimulated by light. The core guided light can couple to SPPs when their phases match. By making the core with high birefringence, the resonance wavelengths of x-polarized and y-polarized mode can be divided. The polarized characteristics are dependent on the parameters of the structure, such as the thickness of metal film and the diameters and positions of the air holes coated metal film. Zhang *et al.* have coated the air holes selectively to realize a absorptive
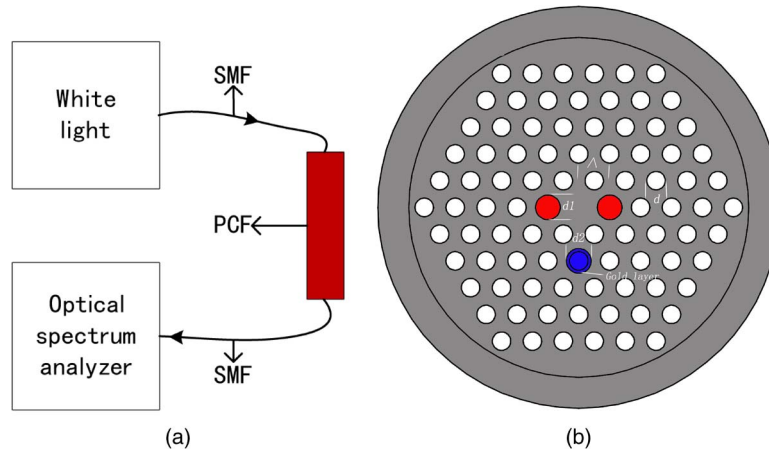
Fig. 1. Schematic of PCF polarized filter system (a) and the cross section of the proposed PCF coated gold film (b).

polarizer [9]. Lee *et al.* have reported a polarization-maintaining PCF with a metal wire, but the resonance wavelengths of two polarized modes are not divided [10]. The PCF with a metal wire has been fabricated by pumping molten metal into the air holes at high pressure [11]. Du*et al.* have reported the polarization-filter characteristics based on high-birefringence PCF with metal wires, the losses of unwanted polarized modes at the wavelength 1.31, 1.55 μm are about 60, 40 dB/cm [12]. Chen *et al.* have proposed a PCF wavelength splitter coated metal film, the losses of unwanted polarized modes at the wavelength 1.31, 1.55 μm are about 102.6, 245.0 dB/m [13]. However, these fibers do not have sufficient performances for the polarized filter.

In this work, polarized characteristics of PCF coated nanoscale gold film are evaluated by a finite element method (FEM). The different filling styles are discussed. The resonance wavelengths of x-polarized and y-polarized mode are divided by making the core with high-birefringence. The resonance wavelengths are adjusted by changing the diameter of the air hole coated gold film. Four kinds of polarized filters based on PCF are realized. We also demonstrate when the diameter of the air hole coated gold film is big enough, the loss of y-polarized mode is further larger than the loss of x-polarized mode in the wide wavelength range.

2. Geometry and Numerical Method

Fig. 1(a) shows the schematic of the PCF polarized filter system. The white light is stable, continuous and broadband light. The upper standard single-mode fiber (SMF) is used to connect white light and PCF. The lower standard single-mode fiber (SMF) is used to connect PCF and optical spectrum analyzer. The cross section of the proposed filter based on PCF coated gold film is shown by Fig. 1(b). The core is formed by removing an air hole. The air holes are arranged in a triangular lattice. The lattice pitch is represented by $\Delta = 2$ μm. The diameters of red holes, blue hole and the other holes are represented by d_1, d_2, and d, and d is fix to 1.2 μm. The blue hole is coated with gold film. Gold will not occur chemical reaction with most chemicals and shows strong corrosion resistance. The ductility of gold is the highest. Filter's bandwidth with gold film is better than that with Ag or Al film [14]. The thickness of gold film is represented by t, and t is fix to 40 nm. The background material is pure silica. Its chromatic dispersion is calculated by the Sellmeier equation [15]. The refractive index of air is 1. The permittivity of the gold is calculated by the Drude-Lorentz model [16]

$$\varepsilon_m = \varepsilon_\infty - \frac{\omega_D^2}{\omega(\omega - j\gamma_D)} - \frac{\Delta\varepsilon \cdot \Omega_L^2}{(\omega^2 - \Omega_L^2) - j\Gamma_L\omega} \tag{1}$$

where ε_∞ is the permittivity in the high frequency, $\varepsilon_\infty = 5.9673$, ω_D is the plasma frequency, $\omega_D/2\pi = 2113.6$ THz, γ_D is the damping frequency, $\gamma_D/2\pi = 15.92$ THz, ω is the angular
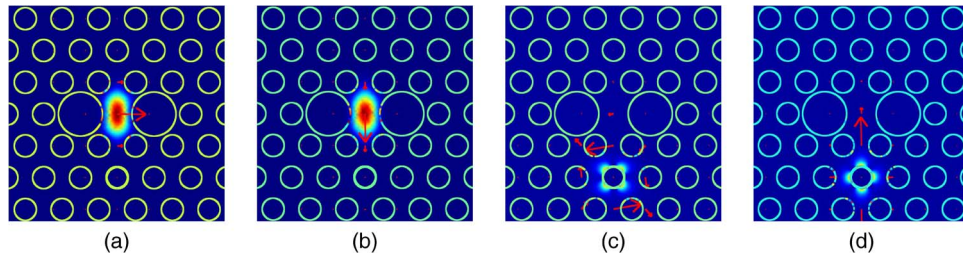
Fig. 2. Electric field distributions of (a) x-polarized (b) y-polarized core mode and (c) x-polarized (d) y-polarized SPP mode.

frequency of transmitting light, $\Delta\varepsilon$ can be regarded as a weighting factor, $\Delta\varepsilon = 1.09$, Ω_L and Γ_L represent the frequency and the spectral width of the Lorentz oscillator, $\Omega L/2\pi = 650.07$ THz, and $\Gamma_L/2\pi = 104.86$ THz. The mode loss of fiber can be calculated by

$$\alpha(x, y) = 8.686 \times \frac{2\pi}{\lambda} \text{Im}(n_{\text{eff}}) \times 10^6 \tag{2}$$

where the unit of the loss and wavelength is dB/m and micrometer, respectively, and $\text{Im}(n_{\text{eff}})$ represents the imaginary part of the effective refractive index of mode.

Nowadays, the fabrication techniques for the perform of PCF include ultrasonic drilling, cast rod in tube, extrusion, and stacking. One metallic coating method involves suction and evaporation of metal nanoparticle mixtures into the fiber. Another method is chemical deposition via precipitation from a reduction reaction. Therefore, the PCF filter coated metal film with simple structure can be fabricated in reality.

The finite element method is used to investigate the mode characters and find the propagation constants of the core modes and plasmonic modes. Perfectly Matched Layer (PML) is used. PML can absorb radiant energy incident at various angles and not reflect energy. In the simulation, cylindrical coordinate is used for PML to absorb the radiant energy from fiber axis. Scattering boundary condition (SBC) is used for the outer boundary of PML. SBC can further reduce reflecting energy. The triangular sub-domain is used to discretize the computation area. The computational region is meshed into 18690 elements for the original structure: $d_1 = 2.4$ μm, and $d_2 = 1.2$ μm.

3. Coupling Theory

At first, a coupling between core mode and SPP mode is analyzed to understand the properties of mode coupling. In this section, $d_1 = 2.4$ μm, and $d_2 = 1.2$ μm. Fig. 2 shows the electric field distributions of core and SPP modes. Fig. 3(a) shows the real part of the effective refractive index dependence on the operating wavelength λ for y-polarized mode. The illustrations of mode field distributions are in the Fig. 3(a). The core mode and SPP mode couple each other and split into another new modes. For lower cure, mode field is mainly distributed in the core-region at the short wavelength, more field begins to transfer from core-region to gold-film-region as wavelength increases, the field intensity in the core-region is same as the field intensity in the gold-film region at the turn of the cure, and almost all the field transfers from core-region to the gold-film-region at the long wavelength. The transition of the upper curve is contrary to that of the lower curve. Fig. 3(b) shows the loss dependence on the operating wavelength λ for y-polarized mode. The transition from core mode to SPP mode also happens to the losses. For the red solid curve, the mode loss follows SPP mode at the short wavelength, and follows core mode at the long wavelength. There is an intersection between the red solid curve and the black dot curve. The losses of the two modes are equal at the intersection. The intersection corresponds to the turn of the cure in Fig. 3(a). This coupling is called complete coupling.

Fig. 4(a) shows the real part of the effective refractive index dependence on the wavelength λ for x-polarized mode. The illustrations of mode field distributions are represented in Fig. 4(a). The core
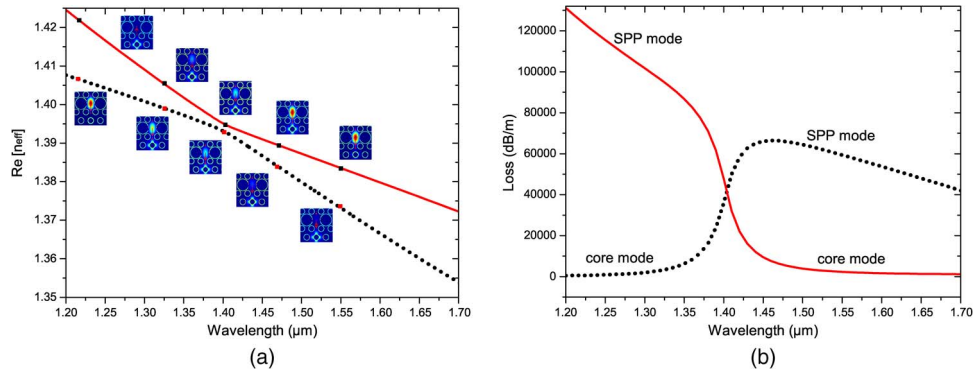
Fig. 3. Real part of the mode refractive effective index (a) and loss of the mode (b) dependence on wavelength when a complete coupling happens. The insets show the electric field distributions of the coupled modes. For lower cure (a), the mode field is mainly distributed in the core-region at the short wavelength, more field begins to transfer from core-region to gold-film-region as wavelength increases, and almost all the field transfers from core-region to the gold-film-region at the long wavelength. The transition of the upper curve is contrary to that of the lower curve.
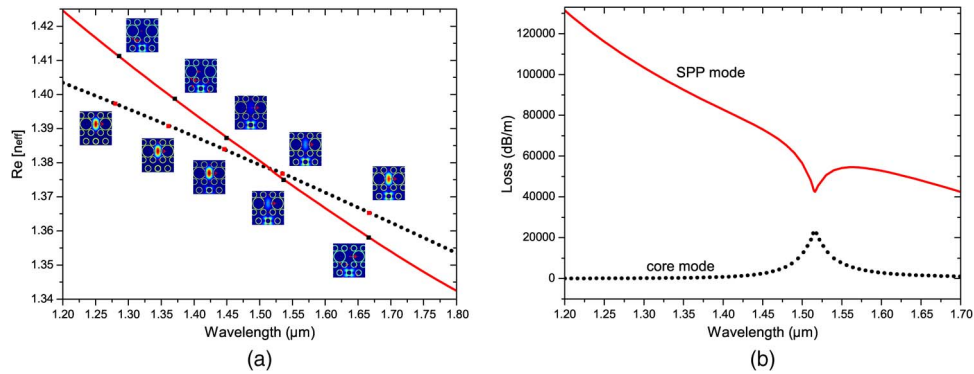

Fig. 4. Real part of the mode effective refractive index (a) and loss of the mode (b) dependence on wavelength when a incomplete coupling happens. The insets show the electric field distributions of the coupled modes. The core mode and SPP mode are confined in core-region and gold-film-region at the short wavelength. Just a little of the mode field of the core couples to the SPP mode as the wavelength increases. Just a little of the SPP mode field couples to the core mode as the wavelength increases. At the longer wavelength, mode fields of the core and SPP modes return to their respective region.

mode and SPP mode are confined in core-region and gold-film-region at the short wavelength. Just a little of the mode field of core couples to the SPP mode as the wavelength increases. Just a little of the SPP mode field couples to the core mode as the wavelength increases. At the longer wavelength, mode fields of the core and SPP modes return to their respective region. Fig. 4(b) shows the loss dependence on the operating wavelength λ for x-polarized mode. At the phase matching point, the losses of core mode and SPP mode are not equal, the loss of core mode is the maximum and the loss of SPP mode is the minimum. This coupling is called incomplete coupling.

Next, we use coupled-mode theory [17] to explain the above phenomena. For core and SPP mode, the coupled-mode equations are

$$\frac{dE_1}{dz} = i\beta_1 E_1 + i\kappa E_2 \tag{3}$$

$$\frac{dE_2}{dz} = i\kappa E_1 + i\beta_2 E_2 \tag{4}$$

where β_1 and β_2 are the propagation constants of core and SPP mode, E_1 and E_2 are the mode fields of the two modes, κ is the coupling strength, and z is the propagation length. We assume

the propagation constant of the coupling mode is β. E_1 and E_2 can be represented by the following equations:

$$E_1 = A\exp(i\beta z) \tag{5}$$

$$E_2 = B\exp(i\beta z). \tag{6}$$

We substitute (5) and (6) into (3) and (4) and get β

$$\beta_\pm = \beta_{ave} \pm \sqrt{\delta^2 + \kappa^2} \tag{7}$$

where $\beta_{ave} = (\beta_1 + \beta_2)/2$, and $\delta = (\beta_1 - \beta_2)/2$. The two modes are leaky because their real parts of mode refractive index are lower than that of the background material. For leaky modes, β_1 and β_2 are complex. Therefore, δ can be represented by $\delta = \delta_r + i\delta_i$. The real parts of propagation constants of core and SPP mode are equal as phase matching condition is satisfied; therefore, $\delta_r = 0$. Then, we can get the equation

$$\delta^2 + \kappa^2 = -\delta_i^2 + \kappa^2 \tag{8}$$

when $\delta_i < \kappa$, the real parts of β_+ and β_- are different, the imaginary parts of β_+ and β_- are equal, and a complete coupling happens as y-polarized mode. When $\delta_i > \kappa$, the real parts of β_+ and β_- are equal, the imaginary parts of β_+ and β_- are different, a incomplete coupling happens as the x-polarized mode.

4. Polarization Filter

4.1. Comparing With Different Filling Style

Fig. 5 shows the loss dependence on the operable wavelength λ for x-polarized and y-polarized mode of core; in this part, d_2 is fix to 1.2 μm. In Fig. 5(a), $d_1 = 2.4$ μm, the resonance wavelengths of x-polarized and y-polarized mode are 1.516 and 1.40 μm, respectively, the corresponding losses are 23 644 and 36 094 dB/m, and the loss of x-polarized mode is just 812 dB/m at the wavelength 1.40 μm. In Fig. 5(b), $d_1 = 1.2$ μm, the resonance wavelengths of x-polarized and y-polarized mode are all 1.227 μm, and the corresponding losses are 883 and 5632 dB/m, the loss of y-polarized mode is larger than the loss of x-polarized mode at the resonance wavelength, because the air hole coated gold film is in y-direction, and y-polarized mode couples to SPP mode easier than x-polarized mode. Comparing Fig. 5(a) with Fig. 5(b), we find the resonance wavelengths of x-polarized and y-polarized mode are divided by increasing d_1 because the difference of the effective refractive index between x-polarized and y-polarized mode exists, and the corresponding losses are increased because the polarized modes are extruded to the y-direction.

Fig. 5(c) shows the loss dependence on the wavelength λ based on the PCF with two air holes coated gold film, the structural parameters of the two air holes coated gold film are the same, $d_1 = 2.4$ μm, the resonance wavelengths of x-polarized and y-polarized mode are 1.516 and 1.40 μm respectively, the corresponding losses are 33 732 and 39 139 dB/m, and the loss of x-polarized mode is 1595 dB/m at the wavelength 1.40 μm. Fig. 6(a) and (b) shows the electric field distributions of x-polarized mode at the wavelength 1.516 μm and y-polarized mode at the wavelength 1.40 μm. Comparing Fig. 5(a) with Fig. 5(c), we find the losses of the PCF with two air holes coated gold film at the resonance wavelengths are all increased, and the loss of x-polarized mode at the wavelength 1.40 μm is also increased.

Fig. 5(d) shows the loss dependence on the wavelength λ with single gold wire, $d_1 = 2.4$ μm, the diameter of metal wire is $d_2 = 1.2$ μm, the resonance wavelengths of x-polarized and y-polarized mode are 1.63 and 1.505 μm, respectively, the corresponding losses are 16 805 and 22 447 dB/m, and the loss of x-polarized mode at the wavelength 1.505 μm is 600 dB/m. Fig. 6(c) and (d) shows the electric field distributions of x-polarized mode at the wavelength

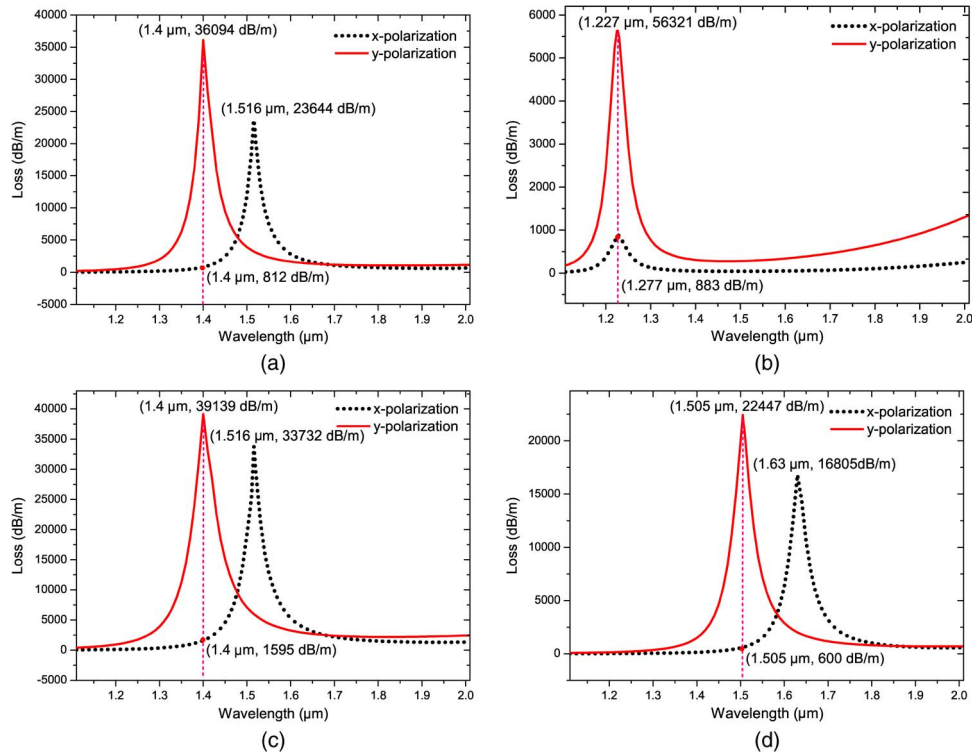Fig. 5. Loss dependence on the wavelength with one air hole coated gold film $d_1 = 2.4$ μm (a), one air hole coated gold film $d_1 = 1.2$ μm (b), two air holes coated gold film $d_1 = 2.4$ μm (c), one air hole filled gold wire $d_1 = 2.4$ μm, and the diameter of gold wire is 1.2 μm (d).
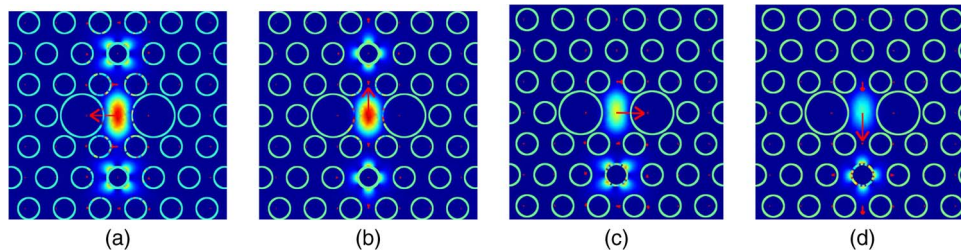

Fig. 6. Electric field distributions of x-polarized mode (a) at the wavelength $\lambda = 1.516$ μm, y-polarized mode (b) at the wavelength $\lambda = 1.4$ μm with two air holes coated gold film, $d_1 = 2.4$ μm, and x-polarized mode (c) at the wavelength $\lambda = 1.63$ μm, y-polarized mode (d) at the wavelength $\lambda = 1.505$ μm with one air hole filled gold wire, $d_1 = 2.4$ μm, and the diameter of gold wire is 1.2 μm.

1.63 μm and y-polarized mode at the wavelength 1.505 μm. The electric field distributions are similar to those in Fig. 2. Comparing Fig. 5(a) with Fig. 5(d), we find the losses of the PCF with gold wire at the resonance wavelengths are all decreased, and the loss of x-polarized mode at the resonance wavelength of y-polarized mode is also decreased.

For polarization filter, we hope not only the loss of wanted polarized mode small but also the loss of unwanted polarized mode big. Therefore, the structural style of Fig. 5(a) is what we want. Next, we introduce single wavelength polarization filters.

4.2. Single Wavelength Polarization Filter

In this section, d_1 is fix to 2.4 μm. We realize the polarization filters based on PCF by modulating the diameter of the air hole coated gold film. For the filter in Fig. 7(a), the diameter of the
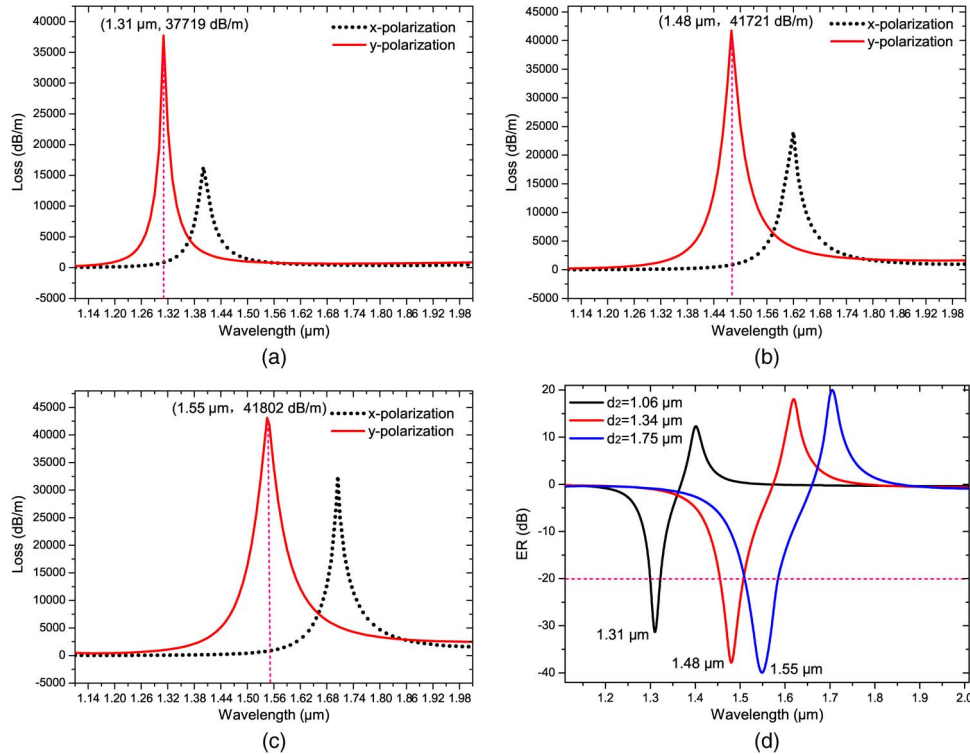
Fig. 7. Loss with (a) $d_2 = 1.06$ μm, (b) $d_2 = 1.34$ μm, (c) $d_2 = 1.5$ μm, and (d) ER dependence on the wavelength. (a) Filter for 1.31 μm. (b) Filter for 1.48 μm. (c) Filter for 1.55 μm. (d) ER.

air hole coated gold film is 1.06 μm, the resonance wavelength of y-polarized mode is 1.31 μm, the corresponding loss is 37 719 dB/m better than [12] and [13]. For the filter in Fig. 7(b), the diameter of the air hole coated gold film is 1.34 μm, the resonance wavelength of y-polarized mode is 1.48 μm, the corresponding loss is 41 721 dB/m. For the filter in Fig. 7(c), the diameter of the air hole coated gold film is 1.5 μm, the resonance wavelength of y-polarized mode is 1.55 μm, and the corresponding loss is 41 802 dB/m better than [12] and [13]. To show loss relation between x-polarized and y-polarized mode, extinction ratio (ER) is introduced which can be calculated by

$$ER = 10 * \lg \frac{P_y}{P_x}. \tag{9}$$

ER is shown by Fig. 7(d) as fiber length is assumed to be 1 mm. The two modes can be divided very well when ER is better than -20 dB.

4.3. Wide Wavelength Polarization Filter

From Fig. 7, we find the full width at the half-minimum of the loss curve increase with the increasing d_2. Therefore, we try increasing d_2 to realize broadband polarization filter. Fig. 8(a) shows the loss of x-polarized and y-polarized mode of core dependence on the wavelength λ based on polarization filter for wide wavelength, the structural parameters are $d_1 = 2.4$ μm, $d_2 = 2.4$ μm, $d = 1.2$ μm, and $t = 40$ nm. The loss of y-polarized mode is better than 35 000 dB/m in the wavelength range 1.25–2.0 μm, the corresponding loss of x-polarized mode is small. The losses of y-polarized mode are 68 576, 64 991, and 47 702 dB/m at the wavelength 1.27, 1.37, and 1.74 μm, respectively, and the corresponding electric field distributions are shown by Fig. 9. The electric field distributions of SPP modes are not similar to those shown by Fig. 2. And the number of SPP modes increases. The y-polarized mode of core couples to different
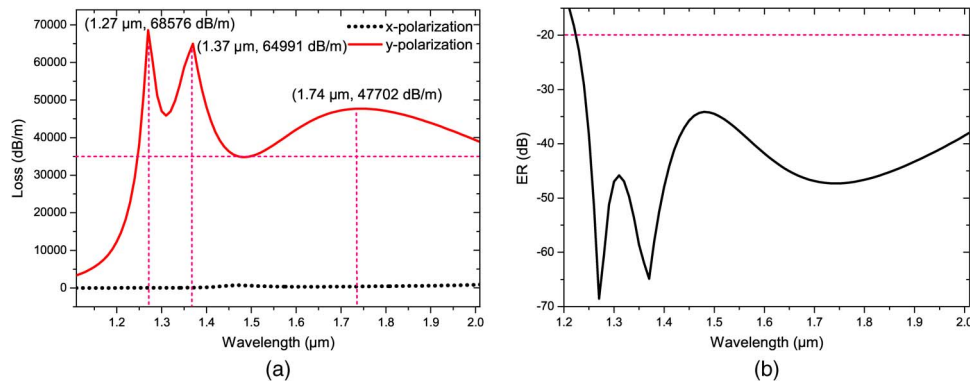
Fig. 8. (a) Loss and (b) ER dependence on the wavelength with $d_1 = 2.4$ μm, $d_2 = 2.4$ μm, $d = 1.2$ μm, and t = 40 nm. (a) Filter for wide wavelength. (b) ER.
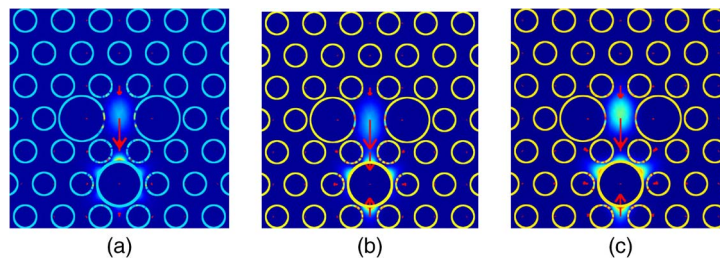

Fig. 9. Electric field distributions of y-polarized mode at the wavelength (a) $\lambda = 1.27$ μm, (b) $\lambda = 1.37$ μm, and (c) $\lambda = 1.74$ μm for filter of wide wavelength.

SPP modes; therefore, Fig. 8 shows three peaks. ER is shown by Fig. 8(b) as fiber length is assumed to be 1 mm.

Finally, the tolerance of realistic fabrication is analyzed. We calculate the impacts of the slight changes in the diameters of air holes and the thick of gold film on the loss spectra. Numerical simulations reveal that the PCF filter for wide wavelength has a relatively strong tolerance of realistic fabrication. Fig. 10 shows the loss spectra of y-polarized mode of core are slightly affected as the diameters of air holes fluctuate 20 nm and the thick of gold film fluctuates by 10 nm. We find the loss spectra are more sensitive to the thick of metal film than the diameters of the air holes. When the thick of metal film decreases, the loss spectra red-shift, and the values of losses increase in a wide wavelength range. The broadband polarization filter provides a better tolerance of realistic fabrication.

5. Conclusion

We propose two kinds of polarization filters with nanoscale gold film for 1.31-μm, 1.48-μm, 1.55-μm, and wide wavelength based on a finite element method. The coupling theory of core mode and SPP mode are introduced. By modulating the birefringence of core, the resonance wavelengths of x-polarized and y-polarized mode are divided. The loss of PCF with gold film is larger than the loss of PCF with gold wire at the resonance wavelength. Compared with the PCF with two air holes coated gold film, the PCF with one air hole coated gold film is more suitable as polarization filter. By modulating the diameter of the air hole coated gold film, we realize four polarization filters based on PCF. When the diameter of the air hole coated gold film is 2.4 μm, the loss of y-polarized mode is better than 35000 dB/m in the wavelength range 1.25–2.0 μm. The broadband polarization filter covering 750 nm with gold film is proposed for the first time.
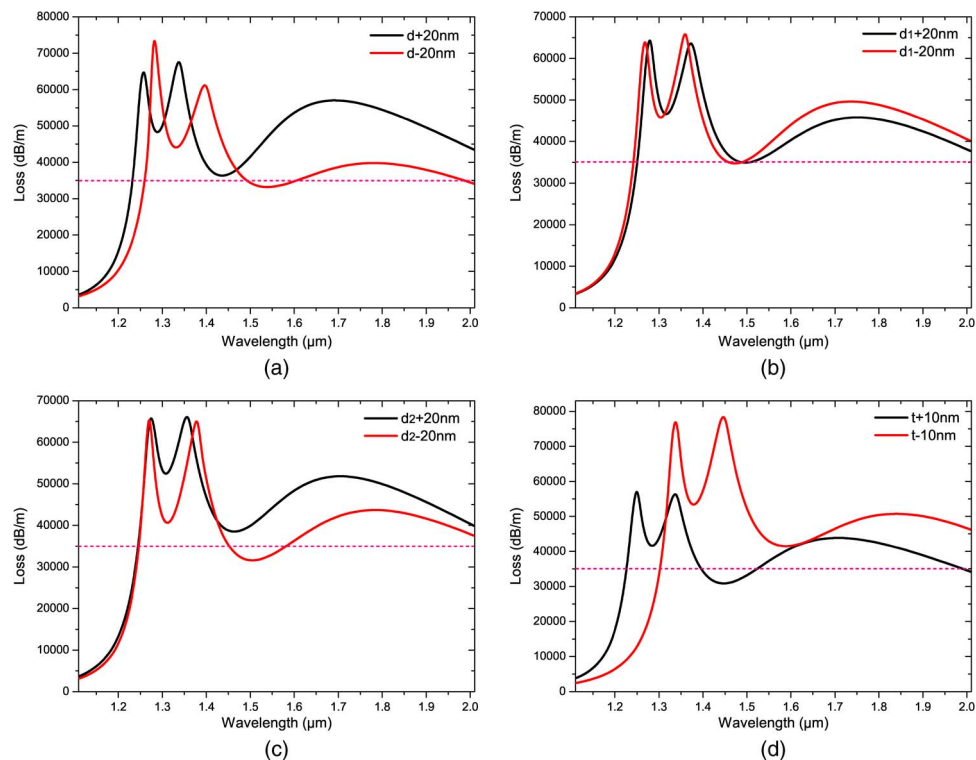
Fig. 10. Loss tolerance of realistic fabrication for y-polarized mode as structural deformation is considered.

Acknowledgment

References

[1] P. St. J. Russell, "Photonic crystal fibers," *J. Lightw. Technol.*, vol. 24, no. 12, pp. 4729–4749, Dec. 2006.

[2] K. Saitoh and M. Koshiba, "Photonic bandgap fibers with high birefringence," *IEEE Photon. Technol. Lett.*, vol. 14, no. 9, pp. 1291–1293, Sep. 2002.

[3] K. Tajima, J. Zhou, K. Nakajima, and K. Sato, "Ultralow loss and long length photonic crystal fiber," *J. Lightw. Technol.*, vol. 22, no. 1, pp. 7–10, Jan. 2004.

[4] T. Matsui, J. Zhou, K. Nakajima, and S. Izumi, "Dispersion-flattened photonic crystal fiber with large effective area and low confinement loss," *J. Lightw. Technol.*, vol. 23, no. 12, pp. 4178–4183, Dec. 2005.

[5] Y. Wang, M. Yang, D. Wang, and C. Liao, "Selectively infiltrated photonic crystal fiber with ultrahigh temperature sensitivity," *IEEE Photon. Technol. Lett.*, vol. 23, no. 20, pp. 1520–1522, Oct. 2011.

[6] H. Chen *et al.*, "A novel polarization splitter based on dual-core photonic crystal fiber with a liquid crystal modulation core," *IEEE Photon. J.*, vol. 6, no. 4, Aug. 2014, Art. ID. 2201109.

[7] S. Zhang *et al.*, "Theoretical study of dual-core photonic crystal fiber with metal wire," *IEEE Photon. J.*, vol. 4, no. 4, pp. 1178–1187, Aug. 2012.

[8] Y. Geng, X. Li, X. Tan, Y. Deng, and X. Hong, "Compact and ultrasensitive temperature sensor with a fully liquid-filled photonic crystal fiber mach-zehnder interferometer," *IEEE Sens. J.*, vol. 14, no. 1, pp. 167–170, Jan. 2014.

[9] X. Zhang, R. Wang, F. M. Cox, B. T. Kuhlmey, and M. C. J. Large, "Selective coating of holes in microstructured optical fiber and its application to in-fiber absorptive polarizers," *Opt. Exp.*, vol. 15, no. 24, pp. 16 270–16 278, Nov. 2007.

[10] H. W. Lee, M. A. Schmidt, H. K. Tyagi, L. Prill Sempere, and P. St. J. Russell, "Polarization-dependent coupling to plasmon modes on submicron gold wire in photonic crystal fiber," *Appl. Phys. Lett.*, vol. 93, no. 11, Sep. 2008, Art. ID. 111102.

[11] H. W. Lee *et al.*, "Pressure-assisted melt-filling and optical characterization of Au nano-wires in microstructured fibers," *Opt. Exp.*, vol. 19, no. 13, pp. 12 180–12 189, Jun. 2011.

[12] Y. Du, S. Li, X. Zhu, and X. Zhang, "Polarization splitter filter characteristics of Au-filled high-birefringence photonics crystal fiber," *Appl. Phys. B*, vol. 109, no. 1, pp. 65–74, Oct. 2012.

[13] L. Chen *et al.*, "Design for a single-polarization photonic crystal fiber wavelength splitter based on hybrid-surface plasmon resonance," *IEEE Photon. J.*, vol. 6, no. 4, Aug. 2014, Art. ID. 2200909.

[14] T. Srivastava, R. Das, and R. Jha, "Highly sensitive plasmonics temperature sensor based on photonic crystal surface plasmon waveguide," *Plasmonics*, vol. 8, no. 2, pp. 515–521, Aug. 2013.

[15] G. P. Agrawal, *Nonlinear Fiber Optics*. San Diego, CA, USA: Academic, 1989.

[16] A. Vial, A. Grimault, D. Maclas, D. Barchiesi, and M. Chapelle, "Improved analytical fit of gold dispersion: Application to the modeling of extinction spectra with a finite-difference time-domain method," *Phys. Rev. B*, vol. 71, no. 8, Feb. 2005, Art. ID. 085416.

[17] Z. Zhang, Y. Shi, B. Bian, and J. Lu, "Dependence of leaky mode coupling on loss in photonic crystal fiber with hybrid cladding," *Opt. Exp.*, vol. 16, no. 3, pp. 1915–1922, Feb. 2008.